H. H. Gorris and D. R. Walt

DOI: 10.1002/anie.200906417

Ultrasmall-Scale Analysis

Analytical Chemistry on the Femtoliter Scale

Hans H. Gorris and David R. Walt**

Keywords:
arrays · fluorescence microscopy · optical-fiber bundles · sensors · single molecules

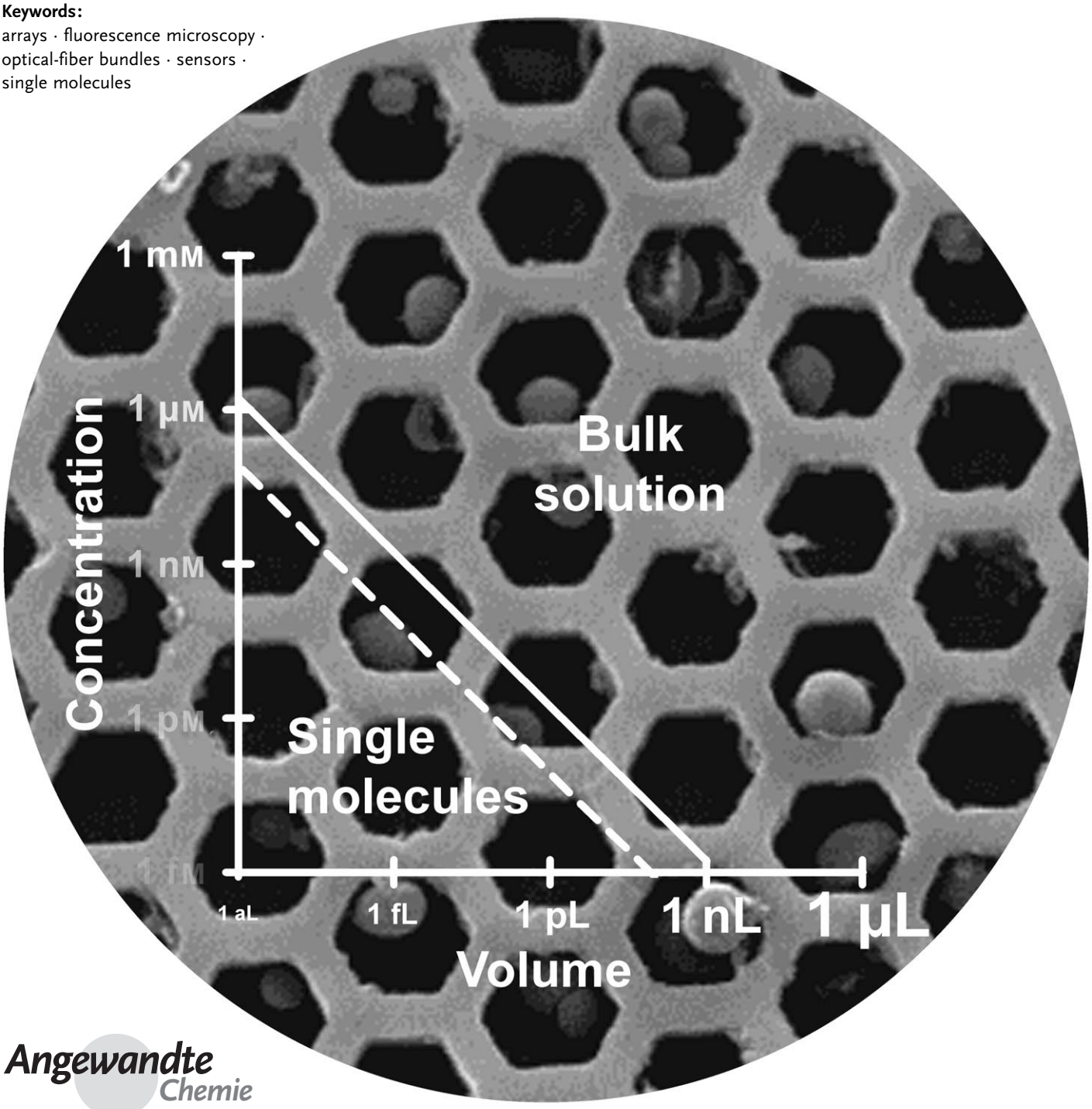

The compartmentalization of reactions in femtoliter (fL) containers and integration of fL containers into arrays not only enhances and accelerates chemical and biochemical analysis but also leads to new scientific methods and insights. This review introduces various fL container and array formats and explores their applications for the detection and characterization of biologically relevant analytes. By loading analytes, sensing elements, or cells into fL arrays, one can perform thousands of analytical measurements in parallel. Confining single enzyme molecules in fL arrays enables one to analyze large numbers of individual enzyme molecules simultaneously in solution. New nanofabrication techniques and progressively more sensitive detection methods drive the field of fL analytical chemistry. This review focuses on the progress and challenges in the field of fL analytical chemistry with examples of both basic and applied research.

From the Contents

1. Introduction

One femtoliter is a volume with dimensions of 1 μm^3, which is the approximate volume of the bacterial cell *Escherichia coli*.[1] Thus, fL containers are at the scale of living cells, with cells even serving as miniaturized test tubes.[2] A free-standing droplet of one fL would evaporate in approximately 5 ms in air;[3] therefore, fL chemistry must be performed in containers to prevent evaporation. New tools and methods are available for designing fL and sub-fL containers that can be used to perform analytical chemistry in ultrasmall volumes.

Section 2 of this review deals with the fabrication and analytical applications of fL containers. Since fL containers measure only a few micrometers in diameter, many thousands of spatially arranged containers can form very high density arrays.[4] Such arrays can be filled with large numbers of sensing elements that can be interrogated simultaneously for multiplexed measurements.[5] Fluorescence microscopy is one of the most sensitive techniques for interrogating analytes in ultrasmall reaction containers. In recent years, advances in photonics technologies such as CCD and CMOS detectors (CCD: charge-coupled device; CMOS: complementary metal oxide semiconductor) have enabled the rapid acquisition of high-resolution fluorescence images with high sensitivity. Large-scale analytical measurements are a requirement for collecting large data sets such as the entire human genome DNA sequence. This information, for example, provides the foundation for the new field of Systems Medicine that integrates the information collected by new analytical technologies. Systems Medicine aims to uncover complex causes of diseases and to find diagnostic biomarkers for diseases.[6]

Femtoliter containers and arrays are particularly important for the emerging fields of single-cell and single-molecule detection, which are described separately in Sections 3 and 4 of this review. Conventional ensemble or bulk experiments can analyze only the average behavior of a population but not the contribution of its individual members. In order to observe heterogeneities in a population, cells or molecules must be monitored individually. Individual living cells can be manipulated or deposited into an array by matching the container size to a particular cell type. The direct deposition of individual molecules of an analyte into fL containers is impractical. An alternative strategy is to fill large arrays of fL containers randomly with a dilute analyte solution. The expected number of molecules in a given volume at a particular concentration is shown in Table 1. Reducing the container volume to 1 fL leads to less than one molecule per container at a concentration of 1 nM. To ensure that a maximum of a single molecule is present in a given container, even lower concentrations are used. Consequently, on average there is less than one molecule present per container and most of the containers are empty. In large arrays of fL containers, however, hundreds or thousands of individual molecules can be monitored simultaneously with wide-field fluorescence microscopy. In pioneering work dating back to 1961, Rotman observed the accumulation of fluorescent product by single enzyme molecules in water-in-oil droplets.[7] With the development of highly homogeneous fL arrays and modern CCD

Table 1: Expected number of molecules in a given volume at a particular concentration.

Volume			1 μM	1 nM	1 pM
$(1\ mm)^3$	1 microliter (μL)	10^{-6} L	6×10^{11}	6×10^{8}	6×10^{5}
$(100\ \mu m)^3$	1 nanoliter (nL)	10^{-9} L	6×10^{8}	6×10^{5}	6×10^{2}
$(10\ \mu m)^3$	1 picoliter (pL)	10^{-12} L	6×10^{5}	6×10^{2}	<1
$(1\ \mu m)^3$	1 femtoliter (fL)	10^{-15} L	6×10^{2}	<1	
$(100\ nm)^3$	1 attoliter (aL)	10^{-18} L	<1		

[*] Dr. H. H. Gorris
Institute of Analytical Chemistry, Chemo- and Biosensors
University of Regensburg
Universitätsstrasse 31, 93040 Regensburg (Germany)
Fax: (+49) 941-943-4064
E-mail: hans-heiner.gorris@chemie.uni-regensburg.de
Prof. Dr. D. R. Walt
Department of Chemistry, Tufts University
62 Talbot Avenue, Medford, MA 02155 (USA)
Fax: (+1) 617-627-3443
E-mail: david.walt@tufts.edu

detectors, it has now become possible to analyze the real-time kinetics of single enzyme molecules.

2. From fL Containers to fL Arrays

Although fL and sub-fL volumes can be confined in various ways, there are two general approaches to preparing arrays of ultrasmall volume containers. The first approach to prepare miniaturized containers is by self-assembly (bottom-up approach), such as emulsions, vesicles, and virus particles. A comprehensive review of self-assembled nanocontainers including containers with volumes much smaller than 1 fL is beyond the scope of this article and can be found elsewhere.[8] Alternatively, ultrasmall containers can be prepared by surface patterning such as etching techniques (top-down approach). Both approaches have been used for designing large arrays. Top-down approaches allow the fabrication of arrays with open microwells that can be filled repetitively. This section of the review introduces different fL container formats and arrays, and discusses various aspects of fL analytical chemistry. Container formats that are important only in the context of single-cell and single-molecule studies will be described in Sections 3 and 4.

2.1. Emulsion-Defined Containers

2.1.1. Standard Emulsions

An easy way to create fL containers is by using water-in-oil emulsions. Standard emulsification methods involve stirring two immiscible liquids such as water and oil in the presence of a surfactant.[9] The size of the water-in-oil droplets is controlled by the agitation. Standard emulsification methods, however, provide little control over the formation of individual droplets, which typically have a broad size distribution.[10]

Standard water-in-oil droplets have served as reaction containers for the polymerase chain reaction (PCR) to amplify DNA specifically from very low concentrations of template DNA. When dilute solutions of DNA template are used and the DNA is distributed over many droplets, the most probable number of templates per droplet is zero, but some of the droplets contain a single copy of DNA. In water-in-oil droplets of 2 to 10 μm in diameter, it is possible to perform PCR with only a single copy of a DNA template molecule.[11] Amplification of complex gene libraries by PCR in emulsified droplets prevents recombination between homologous or partially homologous gene fragments during PCR because one, or at most two, template DNA molecules are present in each droplet of the emulsion (Figure 1).[12] In this way, the

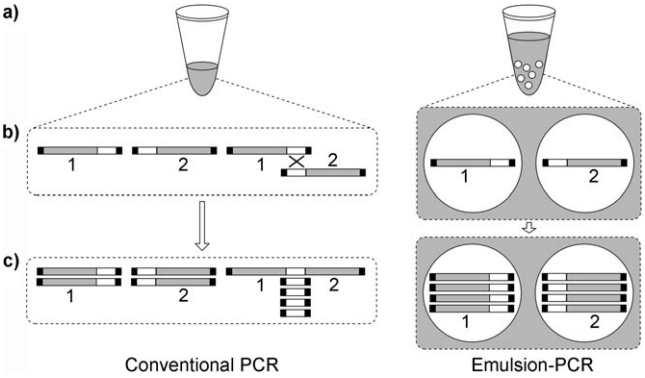

Figure 1. Amplification of complex gene libraries by conventional PCR and emulsion PCR. a) DNA fragments are amplified together in conventional PCR (left) or compartmentalized in emulsified water droplets that contain one, or at most, a few template DNA molecules (right). b) An identical linker (black) ligates to the end of each DNA molecule for amplification with a single PCR primer. In conventional PCR, two template DNA molecules with nonhomologous (gray, 1 and 2) and homologous regions (white) could recombine, leading to the formation of chimeric products. In an emulsion, by contrast, the segregation of template DNA molecules prevents the formation of chimeric products. c) In conventional PCR, the short, chimeric products are amplified more efficiently than the template DNA molecules, leading to a buildup of artifactual DNA, which is avoided in emulsion PCR. Modified schematic representation reprinted with permission from Ref. [12].

synthesis of short, chimeric PCR products and other artifacts can be eliminated. Emulsion PCR was also used for solid-phase DNA sequencing on beads.[13] One DNA template molecule was bound per bead and the beads were then enclosed in emulsified droplets with a PCR reaction mixture. The PCR amplification mix confined in each droplet resulted in beads with millions of identical copies of one DNA molecule template. Subsequently, the emulsion was dissolved

Hans-Heiner Gorris studied biology at the University of Münster and the University of York, England. He designed a high-throughput protease assay in the group of Dr. Andreas Frey at the Institute of Infectiology in Münster and the Research Center Borstel. In 2005 he received his PhD from the University of Lübeck. He then joined the laboratory of Prof. David Walt at Tufts University and worked on single-enzyme-molecule kinetics in optical-fiber bundle arrays. In 2009 Dr. Gorris joined the Faculty of Chemistry and Pharmacy at the University of Regensburg. His research interests include single-molecule enzymology applied to biomedicine and the design of miniaturized assays.

David R. Walt is the Robinson Professor of Chemistry and Howard Hughes Medical Institute Professor at Tufts University. His research group applies micro- and nanotechnology to urgent biological problems such as the analysis of genetic variation and the behavior of single cells, as well as the practical application of arrays to the detection of various analytes including explosives, chemical warfare agents, and food and waterborne pathogens. He is the Founding Scientist, Director and Chairman of the Scientific Advisory Board at both Illumina, Inc. and Quanterix Corporation.

and the beads were subjected to automated sequencing. Water-in-oil droplets with a mean diameter of 2.6 μm (9 fL) were also used for in vitro transcription and translation in a cell-like volume. The droplets contained a transcription/translation reaction mixture for expressing single genes of *HaeIII* methyltransferase.[14] Recently, the enhanced green fluorescent protein (eGFP) was synthesized by cell-free protein expression in water-in-oil droplets with diameters of 1–100 μm.[15]

2.1.2. Droplets Generated by Microfluidics

More homogeneous water-in-oil droplets can be obtained with microfluidic tools. The most common microfluidic arrangements for generating water-in-oil droplets are flow-focusing channels and T-junction channels.[16] In flow-focusing generators, oil flows through two outer channels and an aqueous solution through a central channel. The combined fluids are pressed through a narrow orifice to form monodisperse aqueous droplets in oil.[17] In this way, large numbers of monodisperse pL droplets dispersed in hexadecane[16] or fluorocarbon oils[18] can be generated. Droplets generated by flow-focusing with a volume of 65 pL were used as reaction containers for PCR.[19] Recently, single DNA template molecules in 2 pL droplets were amplified by isothermal rolling circle amplification.[20] A different format involves a microfluidic T-junction, which consists of a main channel containing oil and a second perpendicular channel that inserts an aqueous solution into the oil flow. Monodisperse water-in-oil droplets are generated through shear forces at the T-junction.[21] The combination of T-junction geometry with optical trapping allows the directed deposition of single beads, cells, or subcellular structures into water-in-oil droplets of approximately 90 fL volume.[22] The particles can be moved by optical trapping from an aqueous solution to the interface between the aqueous phase and oil at a microfluidic T-junction. Then, a pressure pulse is applied to the aqueous phase to shear off a droplet that encapsulates a single polystyrene bead, cell, or mitochondrion. Alternatively, an aqueous solution can be pressed through a narrow orifice into an immiscible phase and then pinched off by application of a sudden negative pressure.[23] Droplets with a volume of a few fL were optically trapped and fused to initiate chemical reactions. Optically trapped droplets in oil are also amenable to shrinkage and expansion.[24] With a piezoelectric actuated device, droplets 1–2 μm in diameter (0.5–4 fL) containing eGFP were generated in a perfluorinated immiscible phase.[25] These droplets were subsequently optically trapped and held at the focus of an excitation laser with a confocal microscope. In such small volumes, single-molecule bleaching events of GFP were observable. Finally, a pulsed electric field instead of pressure was applied to generate fL to pL droplets in oil.[26]

2.1.3. Droplets inside Microfluidic Channels

Aqueous droplets inside microfluidic devices can be compartmentalized by inserting an alternating stream of water and a second immiscible fluid into a microfluidic channel. The reactions in microfluidic droplets and their applications have been reviewed previously.[27] The transport of droplets through the channels is analogous to a fluid stream, and the minimal volume of these droplets depends on the minimal channel diameter that allows for effective microfluidic transport. The flow rate in a channel depends linearly on the pressure drop (ΔP), which is given by the Hagen–Poiseuille relation [Eq. (1)].[28]

$$\Delta P = \frac{128 \mu V l}{\pi d^4} \quad (1)$$

Here μ is the viscosity of the fluid, V the volumetric flow rate, l the length of the channel, and d the diameter of the channel. The Hagen–Poiseuille equation applies to single-phase flow. In small droplets, interfacial effects become significant and result in multiphase flow, which increases the pressure drop even further. The pressure drop depends largely on the channel diameter. Consequently, microfluidic channels generally are wider than 10 μm in diameter,[29] such that droplets in microfluidic channels have larger than fL dimensions.

Droplets inside microfluidic devices have found applications for PCR[30] and in vitro transcription and translation of proteins.[31] The in vitro expression of GFP was performed in large numbers of microfluidic droplets with pL volumes. The droplets were generated, incubated, and screened by fluorescence microscopy in integrated microfluidic devices that contained a reservoir for storing approximately 10^6 droplets. A single molecule of DNA template in the microfluidic droplets was sufficient for the in vitro expression of 30000 GFP molecules. In vitro expression of GFP was also performed in fL droplets (Figure 2).[32] By introducing a short constriction into a microfluidic channel, the droplet diameter was reduced to about 5 μm (65 fL).

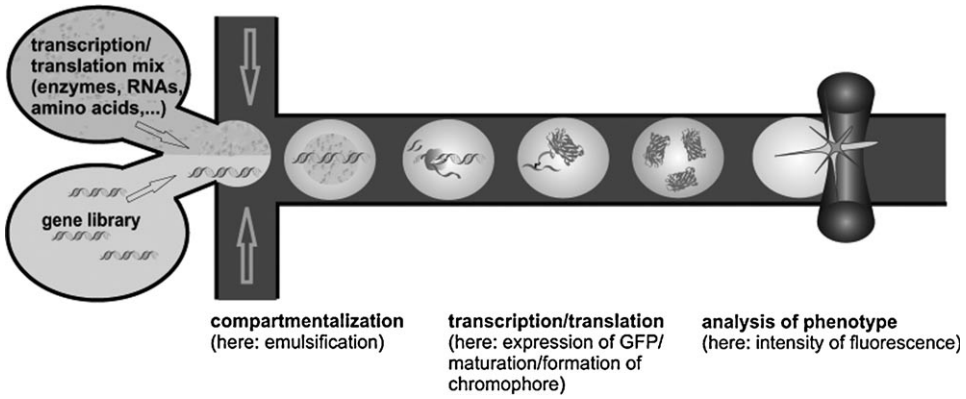

Figure 2. Water-in-oil droplets in a microfluidic channel. The compounds for cell-free expression of proteins are enclosed together with GFP-encoding DNA. DNA is expressed in vitro while the droplets move through the channels. After the GFP chromophore has formed autocatalytically in the droplets, GFP is detectable by fluorescence spectroscopy. Schematic representation reprinted with permission from Ref. [32].

2.1.4. Droplets Generated by Liquid Jets

Monodisperse fL droplets of water coated by olive oil can be generated as aerosols from coaxial liquid jets of immiscible liquids by electrohydrodynamic forces.[33] The electrified jet subsequently breaks up and forms a spray of monodisperse oil-encapsulated water droplets. The flow rates of both liquids and the applied voltage allow precise control over the volume of the water droplets and the thickness of the coating oil layer. The best known application for electrospray is mass spectrometry, where charged ions of biomolecules are contained in the liquid droplets.[34] For mass spectrometry, however, it is essential to evaporate these droplets in vacuo in order to generate ionized biomolecules, while for most other analytical applications, it is essential to prevent evaporation such that the volume of the aqueous droplets remains constant.

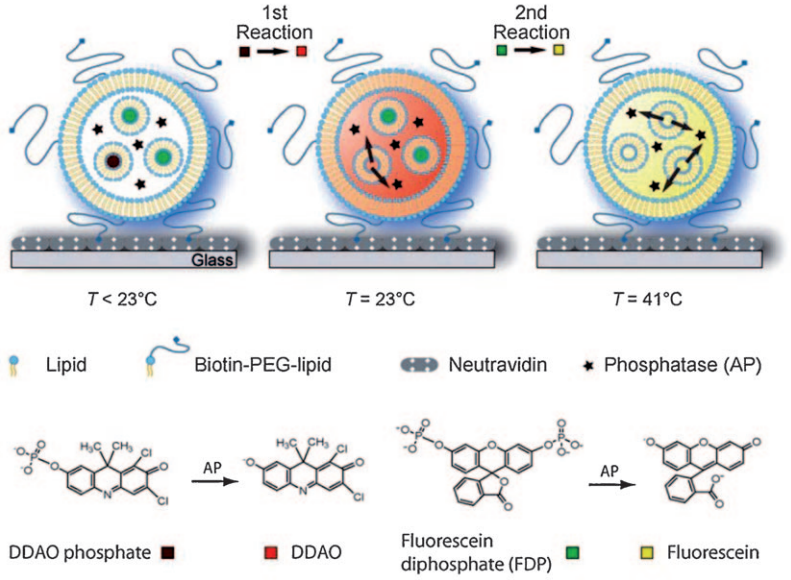

Figure 3. Consecutive enzymatic reactions in a surface-tethered lipid vesicle. Alkaline phosphatase (AP, star) is incorporated in a larger reactor vesicle together with two kinds of smaller lipid vesicles, which are loaded either with dichlorodimethylacridinone (DDAO) phosphate (dark red) or with fluorescein diphosphate (FDP, dark green). At the phase-transition temperatures, the substrates are released into the reactor vesicle, where they are converted by the enzyme to their fluorescent products, DDAO (light red) or fluorescein (light green). Schematic representation reprinted with permission from Ref. [37].

2.2. Lipid Vesicles

In contrast to emulsions, lipid vesicles or liposomes confine a volume by a lipid bilayer, such that the vesicle content as well as the bulk solution are aqueous. There are numerous methods for preparing lipid vesicles. These preparation methods and the applications of lipid vesicles have recently been reviewed.[35] Lipid vesicles can have fL volumes, which are similar to bacterial cells, and both vesicles and cells are confined by lipid bilayers. Owing to these similarities, lipid vesicles are well amenable for investigating the reaction dynamics of biological molecules.

For studying chemical reactions in a biomimetic environment, individual lipid vesicles of 1 to 5 μm in diameter (0.5–65 fL) were optically trapped with an infrared laser or attached to modified glass surfaces.[36] Chemical reactions in these fL containers were investigated by fluorescence microscopy. The reactions were initiated by a short intense electric pulse delivered across ultramicroelectrodes that resulted in either electroporation or electrofusion of the lipid vesicles. Electroporation resulted in an influx of protons. The decreasing pH inside the lipid vesicles containing fluorescein led to fluorescence quenching. Electrofusion of two vesicles was used to mix reagents quantitatively. Two selected vesicles, each containing a different fluorescent dye, were optically trapped and electrofused. The fusion was then analyzed by exciting the mixed contents of the fused vesicle at two different wavelengths.

In an alternative immobilization approach, biotinylated lipid vesicles were tethered to the surface of a neutravidin-coated glass slide (Figure 3).[37] The diameter of the lipid vesicles was varied between 1 and 10 μm (0.5–500 fL). These larger fL reaction vesicles enclosed smaller aL vesicles approximately 100 nm in diameter (0.5 aL). The phase-transition temperatures of the aL vesicle membranes defined the temperature at which the aL vesicles released their cargo into the fL reaction vesicles. Different reactants were released consecutively into the fL reaction container at each phase-transition temperature. The sequential mixing of two non-fluorescent substrates with an enzyme in the fL reaction container initiated the formation of different fluorescent products, which were monitored by fluorescence correlation spectroscopy.

Biotinylated lipid vesicles were also used for self-assembling arrays of surface-tethered containers with an average diameter of 100 nm (0.5 aL).[38] The exposed biotin ligands on the vesicle's surface bound specifically to defined regions on a glass substrate containing immobilized streptavidin. These surface regions were surrounded by areas that prevented nonspecific attachment such that the self-assembling process was guided by the patterned surface functionalization. The size of the array was $0.4 \times 0.4\ mm^2$ with a density of roughly $10^6\ mm^{-2}$. The authors of this study suggested that arrays of lipid vesicle could be used as libraries for the simultaneous screening of millions of analytes or molecular functions while using only pL volumes of reagents.

Lipid vesicles of 10 to 20 μm in diameter (520–4200 fL) were connected by a network of suspended nanochannels (ca. 100 nm in diameter and 20–30 μm in length).[39] This nanofluidic switching device allowed for pumping fL volumes into selected reaction vesicles by manipulating the energy state of the vesicle's lipid bilayer. The nanoscale surfactant networks were used for various analyses such as single-nanoparticle transport, single-DNA-molecule transport, and mimicking exocytosis.[40]

2.3. Nanofiber Junctions

Recently, electrospun polymer nanofibers aligned in a rectangular grid were used to generate arrays of fL to aL volumes (Figure 4).[41] Nanofibers 200 nm in diameter were

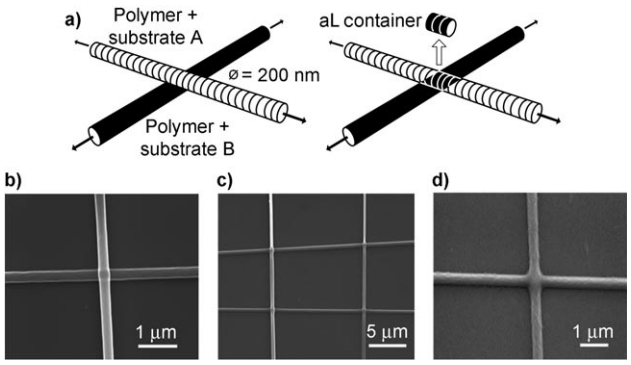

Figure 4. Nanofiber junctions. a) Polymer nanofibers containing different reagents are arranged in a rectangular grid. The reagents are mixed by fusion of the nanofibers. At the junctions, an aL container is created in which as few as 1000 molecules are detectable. Scanning electron microscope (SEM) images of the nanofiber before (b,c) and after fusion(d). Modified images reprinted with permission from Ref. [41].

fused by heat or exposure to solvent vapors to form containers with a volume of 5 aL at the fiber junctions. Fusing two types of nanofibers loaded with different nonfluorescent reactants initiated the formation of a fluorescent reaction product inside the aL containers, which was observable by fluorescence microscopy. 1000 fluorophore molecules were sufficient to yield a detectable signal from these aL containers. Nonfluorescent reaction products were extracted from the fiber junctions and subsequently analyzed by mass spectrometry.

2.4. Optical-Fiber Bundles

Etching techniques allow the direct formation of large numbers of spatially ordered fL containers into surfaces. These tailor-made fL containers form an array, where each fL container has a fixed position. Such arrays avoid problems associated with variations in container sizes and movements of containers. Another advantage for analytical applications is the open container format, with individual containers called microwells. The microwells can be filled with solutions containing analytes after the array fabrication process is finished. The array can also be used repeatedly by rinsing and refilling the microwells.

Our group has pioneered optical-fiber bundles to create high-density arrays (Figure 5).[42] Optical-fiber bundles consist of a few thousands to 100000 individual fiber-optic cores with diameters between 2 and 20 μm that are surrounded by a common cladding material of a lower refractive index than the core material. These fiber-core waveguides transmit optical signals independently by total internal reflection over long distances with low attenuation. The core material

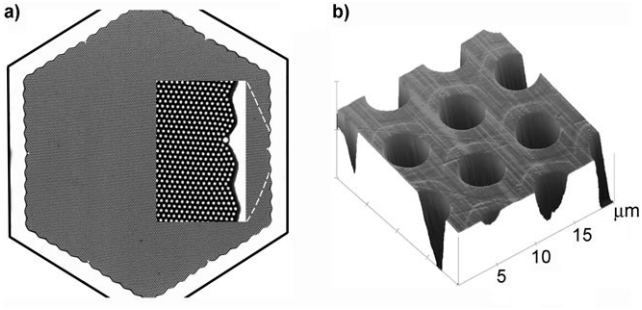

Figure 5. Femtoliter array on an optical-fiber bundle. a) Microscope images of the entire fiber array with an enlarged inset. b) Atomic force microscope image of a portion of the etched surface, showing homogeneous microwells etched with HCl. Modified images reprinted with permission from Ref. [93].

can be acid etched selectively to create an array of uniform fL microwells with a density of approximately 25000 mm^{-2} on one end of the optical-fiber bundle. The microwells are loaded with fluorescent probes. The other end of the fiber bundle is connected to an epifluorescence microscope. To interrogate the wells, excitation light is launched into the entire array. The resulting emission light is captured by the individual cores that define the bottom face of each well. Each fiber core carries only the signal from the microwell to which it is connected. In this manner, one can interrogate tens of thousands of individual reaction containers. The returning emitted light is filtered to remove any scattered excitation light and then detected by a CCD camera.

Microspheres (beads) that match the size of the microwells assemble randomly into the optical-fiber array through capillary forces. Large numbers of beads can be surface modified with sensing elements such as DNA or antibodies, before they are loaded into the array. For DNA analysis, more than 10^{11} beads per gram can be functionalized homogeneously with oligonucleotides and subsequently used for assembling hundreds to thousands of arrays with high reproducibility.[43] The random nature of such arrays requires that each bead must carry an identifier code corresponding to the respective analytical element.[44] In the simplest case, the beads can be optically encoded with one or more fluorescent dyes, and the relative concentrations of the fluorescent labels can serve as an identifier, enabling more codes to be derived from a given set of dyes.[45] The encoding labels must be different from the labels used for the analytical measurement. Direct fluorescent coding is limited by the number of dyes and the concentrations that can be reliably distinguished from each other. An alternative decoding scheme was implemented for oligonucleotide-functionalized beads. The nucleotide sequence on each bead was decoded sequentially into a combinatorial fluorescent code through sequential hybridization/dehybridization cycles with complementary oligonucleotides that carried different fluorophores at each step.[46] This approach enables a much higher number of beads to be used in a random array. This system for decoding oligonucleotide-functionalized beads assembled in an optical-fiber bundle array format as well as planar silicon microwell substrates has been commercialized by Illumina Inc. (San

Diego, USA) for gene expression analysis and genome-wide genotyping of single-nucleotide polymorphisms (SNPs).

Optically encoded beads in optical-fiber bundle arrays were used to detect six biological warfare agents simultaneously.[47] Beads were functionalized with pathogen-specific DNA probes and loaded into the fiber bundle. DNA from autoclaved bacterial pathogens was then isolated and PCR amplified with fluorescently labeled primers. The target DNA of the biological warfare agents was detectable in 30 min with a detection limit of 10 fM. A sandwich-type assay was implemented with the optical-fiber bundle array to detect the foodborne pathogen *Salmonella* spp.[48] Bacterial target DNA was hybridized to capture oligonucleotides on encoded beads. A second fluorescently labeled oligonucleotide signal probe was then hybridized to the target DNA. As the detection of target DNA was dependent on two subsequent recognition events, the specificity of the test was increased. In the presence of the enterobacterium *E. coli*, which has a high DNA sequence similarity, only *Salmonella* spp. was detected selectively. Similarly, three toxin-producing algae species were detected simultaneously by a sandwich assay for ribosomal RNA (rRNA).[49] rRNA is present at more than a million copy numbers per cell. Thus, no amplification steps were required to detect as few as five algal cells. The sandwich-type assay was also amenable to protein detection.[50] In this case, beads were functionalized with capture antibodies specific for immunoglobulin A (IgA) and lactoferrin. A second fluorescently labeled antibody was used for detecting the target proteins with low cross-reactivity.

Finally, DNA and protein detection were combined in a single test.[51] Beads were functionalized with antibodies against the proinflammatory target proteins IL-6 and IL-8. Then, a second biotin-labeled antibody was bound to the target proteins. Biotinylated capture oligonucleotides were attached to the secondary antibodies by means of an avidin linkage. The capture oligonucleotide hybridized a "padlock" DNA. The padlock DNA ligated and formed a circular DNA molecule only when a complementary target DNA strand was present. The circular DNA probe was used for rolling circle amplification, and the amplified sequences were hybridized with complementary fluorescently labeled oligonucleotides. A target DNA was chosen that encoded the outer membrane protein P6 of the respiratory pathogen *Haemophilus influenzae*. A strong fluorescent signal was generated only when proinflammatory proteins were present together with *H. influenzae*.

In a different sensor approach, the microwells of the optical-fiber bundle were filled with cross-reactive beads to design an "artificial nose", based on principles of mammalian olfaction. In contrast to specific recognition elements,[52] cross-reactive sensor beads were prepared that responded to multiple analytes. The beads consisted of different polymers, surface functionalities, and solvatochromic fluorescent dyes.[53] Each type of bead generated a unique fluorescence response pattern to a vapor. The combined array response was then used to train pattern-recognition algorithms that could identify a particular vapor alone and as a component of a complex vapor mixture.[54] Such artificial noses were able to identify various types of coffee-bean odors, as well as explosive vapors.[55] Recently, a portable artificial nose was implemented for in-field detection of arson accelerants.[56]

3. Single Cells in fL Volumes

Living cells are commonly investigated using microtiter well plates, for example, for drug and toxicity screening, cellular sensing, and basic cell biology studies. While assays with microtiter plates monitor only the average response of an entire cell population, single-cell experiments make it possible to observed individual cell responses. Numerous techniques can be used to investigate single cells. Here, three basic types of single-cell experiments in fL volumes will be introduced with examples from the recent literature.

3.1. Cell Sorting in Microfluidic Droplets

Living cells can be encapsulated in microfluidic droplets. Inside a 33 pL droplet, single hybridoma cells were viable for more than 6 h, and they secreted antibodies that accumulated to high concentrations.[57] After the emulsion was dissolved, the antibodies were detected by ELISA. Although the droplet volume could be decreased to approximately 500 fL, these small cell-culture volumes led to decreasing nutrient levels and increasing waste levels, which compromised cell viability. The manipulation of living cells in microfluidic droplets enables a miniaturized class of flow cytometry and fluorescence-activated cell sorting (FACS). A further requirement for automated cell sorting with microfluidic devices is the detection of fluorescent cell markers inside a droplet. Two strains of *E. coli* that differed in the expression of β-galactosidase were enclosed with the fluorogenic substrate fluorescein-di-β-D-galactopyranoside inside microfluidic droplets of 12 pL volume.[58] These bacterial cells could be sorted according to the enzymatic production of the fluorescent product fluorescein. A similar approach was used to analyze surface proteins on single human monocytic cells (Figure 6).[59] The surface proteins were labeled with an antibody-coupled enzyme. The labeled cells were enclosed with fluorescein-di-β-D-galactopyranoside in microfluidic droplets 40 μm in diameter (33 pL). The presence of the cell-surface biomarker was then detectable by the accumulation of fluorescein in individual droplets. Finally, single bacterial cells were tested for their susceptibility to antibiotics in microfluidic droplets of 4 nL.[60]

3.2. Spatially Arranged Cell Deposition

Living bacteria,[61] yeast,[62] and mammalian cells[63,64] can be assembled by sedimentation into the microwells of an optical-fiber bundle. The microwell sizes can be adjusted by using fibers of different diameters to match the sizes of different cell types, which is necessary for cell assembly in the fiber array. Mammalian cells assembled in wells 7 μm in diameter and 3 μm deep (roughly 85 fL).[63] Sustained by a reservoir of nutrients, mammalian cells were viable for more

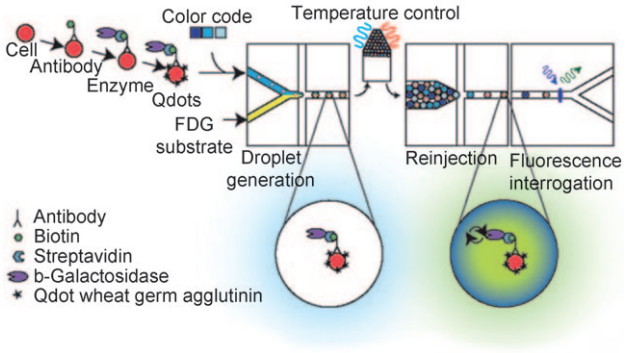

Figure 6. Microfluidic cell sorting. Cell-surface proteins are first labeled with a specific antibody–β-galactosidase conjugate and a lectin-labeled quantum dot. Cells are then encapsulated in microfluidic droplets with a sample-specific color code and the fluorogenic substrate fluorescein-di-β-D-galactopyranoside (FDG). The fluorescein accumulation in each droplet is monitored after a certain incubation time. Schematic representation reprinted with permission from Ref. [59].

than 24 h in the fiber array. Cells were labeled with lipophilic fluorophores,[63] fluorescently labeled lectins,[65] or genetically encoded fluorescent proteins[61,66] to identify them by fluorescence microscopy. The cells were used for the functional screening of biologically active compounds and for analyzing cellular events at the single-cell level. In virtually all cases, a distribution of responses was observed, even from cells that had the same genetic makeup, attesting to the value of single-cell measurements.

Other arrays for single-cell experiments were designed indirectly by lithography and molding techniques. The indirect fabrication method has the advantage that many replicates can be made from a single master stamp. A large array of over 30000 microwells 10 μm in width and 12 μm in depth (approximately 940 fL) was molded in polystyrene to accommodate single lymphocytes.[67] Stimulation of B-cells in the array with an antigen led to an individual response from each cell. Activation of antigen-specific B-cells was detected with the fluorescent Ca^{2+} indicator Fluo-4. The antigen-specific B-cells were then retrieved from the array by a micromanipulation pipet.

Soft lithography is another indirect method for creating arrays of fL wells, where a master mold is used as a template to cast complementary structures in an elastomeric polymer, most commonly poly(dimethylsiloxane) (PDMS).[68] PDMS is nontoxic and O_2-permeable. PDMS arrays of roughly 10000 microwells with varying pL volumes were used to enclose adherent fibroblasts as well as non-adherent leukemia cells.[69] For fluorescence imaging, cell-permeable Calcein AM was added to the cells in the microwells. Esterases in the cytoplasm catalyze the reaction of the nonfluorescent Calcein AM to a fluorescent product. This reaction is specific for living cells because dead cells do not retain active esterases. PDMS arrays of approximately 20000 wells with pL volumes were used to isolate single pheochromcytoma cells from rats.[70] These cells were lysed individually in the microwells to determine intracellular protein concentrations or enzymatic activities. Cells expressing the recombinant fusion protein FLAG-GST were lysed in the presence of surface-immobilized antibody-labeled beads in the PDMS container. In this sandwich-type assay, the antibodies captured FLAG-GST. The PDMS array was then opened to detect FLAG-GST on the beads by means of a fluorescently labeled secondary antibody. For determining enzymatic activities of the intracellular proteases calpain and caspase 3, cells were lysed in the presence of respective fluorogenic substrates. The substrate turnover was then determined from the formation of fluorescent product. It was demonstrated that this simple array in PDMS is suitable for investigating the biochemical characteristics of single cells without complex microfluidic devices.

Lithographically fabricated arrays of microwells (50 μm diameter, 10 μm depth) in the resin SU-8 covered by a microfluidic PDMS channel were used for analyzing quorum-sensing behavior.[71] Quorum sensing helps bacteria coordinate their behavior and is activated when a chemical signal accumulates to a high concentration, which naturally occurs when bacteria are at a high density. Quorum sensing in *Pseudomonas aeruginosa* was detected by the expression of the GFP gene, which was used as a reporter for the quorum-sensing-controlled gene *lasB*. A low-density culture of bacterial cells was delivered through the PDMS channel. When air was driven subsequently through the channel, one to three bacteria were isolated in confined 100 fL droplets in the array. In such small confinements, even a single bacterial cell built up chemical concentrations quickly enough to initiate quorum sensing.

3.3. Single Cells as Reaction Containers

Living cells can be considered to be fL reaction containers.[2] Cells are confined by a lipid bilayer and, in this respect, are similar to lipid vesicles. In living cells, the behavior of single biomolecules can be studied in a more physiological context. This feature is important as biochemical reactions in the cell often occur under non-equilibrium conditions and interact in complex networks. Single-molecule studies in living bacterial cells have enabled new insights into gene regulation, transcription, translation, and replication.[72]

4. Single-Molecule Detection in fL Volumes

The emergence of new techniques and progressively more sensitive detection methods for analyzing enzymes and other biomolecules at the single-molecule level has greatly expanded our understanding of fundamental biochemical mechanisms, which were previously hidden in bulk reactions. For single-molecule experiments, it is important to minimize the volume containing the single molecule of interest so that it can be localized with a high level of confidence. There are two basic formats for performing single-molecule studies of enzyme catalysis using fluorescence microscopy. Single enzyme molecules can be either surface immobilized or spatially constrained by compartmentalization in fL and sub-fL containers, such as emulsion droplets, lipid vesicles, virus

capsids, or surface-etched arrays of fL containers. A hybrid method combines both of these single-molecule formats. For example, single enzyme molecules can be surface immobilized in fL containers or at the bottom of fL wells.

In this review we include techniques that involve surface-immobilized enzymes in ultrasmall containers and wells, while other single-molecule experiments with immobilized enzymes are covered only briefly. As experiments with immobilized enzyme molecules monitor a small number of fluorophore molecules, the excited volume must be small to reduce background contributions arising from fluorescent impurities and Raman scattering. In a decreasing excitation volume, the signal of a single fluorophore is constant, while the background decreases linearly.[73] Confocal and total-internal reflection (TIRF) microscopy are most commonly used for reducing the excitation volume. Individual horseradish peroxidase, β-galactosidase, λ-exonuclease, and lipase molecules were all immobilized to a surface.[74] Alternatively, cholesterol oxidase was immobilized in an agarose gel[75] and GFP in a polyacrylamide gel[76] to prevent them from diffusing.

Single-molecule experiments with immobilized enzymes can be used to monitor sequential catalytic cycles over time and analyze the waiting times required to complete the cycles. While individual waiting times are stochastic events, their statistical properties are determined by the underlying catalytic mechanism. Such single-molecule analyses have revealed dynamic fluctuations in sequential catalytic cycles that can be attributed to conformational changes in the enzyme.[75,77]

For the second type of single-molecule experiment, enzyme molecules are spatially constrained in containers; this has the advantage that steric hindrance, partial inactivation, and perturbation of the enzyme structure resulting from surface immobilization are avoided.[78] Decreasing the container volume reaches a limit where statistically one enzyme molecule is present per container (Figure 7). For fL containers, the single-molecule concentration limit lies in the picomolar range. As the direct deposition of a single enzyme molecule into each fL container is impractical, large arrays of fL containers can be filled randomly with a dilute enzyme solution. At the single-molecule concentration limit, however, each container will not necessarily have exactly one enzyme molecule because of statistical fluctuations. The Poisson distribution describes the probability of a rare event occurring in a large number of trials. The probability $P_\mu(x)$ that a container contains exactly x enzyme molecules is given by Equation (2), where μ is the average number of enzyme molecules per container.

$$P_\mu(x) = \frac{e^{-\mu}\mu^x}{x!} \quad (2)$$

The Poisson distribution is a simple statistical way to determine how to maximize the number of fL containers containing a single enzyme molecule. For example, a 1:20 ratio of enzyme molecules to containers results in 95% empty containers, 5% single molecules, and only 0.1% with more than a single enzyme molecule. Decreasing the concentration further to reduce the probability of multiple molecules per container comes at the price of increasing the number of empty containers. Thus, this approach is practical only if arrays with large numbers of fL containers are available.

A fluorogenic substrate can simply be added to the dilute enzyme concentration and enclosed in the array. The substrate concentration is much higher than the enzyme concentration, and the term "single-molecule experiment" refers only to the enzyme. If desired, the substrate concentration can be varied to investigate different reaction conditions. While each fL container holds the same amount of substrate, the fluorescent product is observed only in those containers that contain a single enzyme molecule. As the activity of only a single enzyme molecule is observed, it is not necessary to know the exact concentration of the bulk enzyme solution, which is a critical parameter for calculating the turnover number k_{cat} in traditional bulk reactions. The single-molecule approach eliminates the need to know the fraction of active enzymes in an enzyme preparation and renders such compromises as the definition of enzyme units superfluous. Furthermore, it is convenient to replace the molarity of the substrate and the product solution by the total number of molecules in the confined fL volume to have a direct measure of turnover rates. For example, a typical 100 μM substrate concentration confined in a fL volume corresponds to a few million substrate molecules.

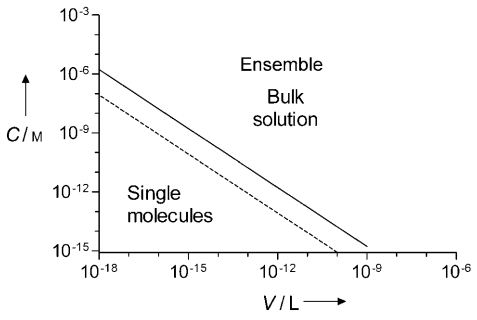

Figure 7. The single-molecule concentration limit. The concentration (C) that yields, on average, one molecule per container (solid line) is inversely dependent on the container volume (V). The actual occupancy with molecules is given by the Poisson distribution [Eq. (2)]. A 1:20 ratio of molecules to containers (hatched line) results in 95% empty containers, 5% with a single, and only 0.1% with two or more molecules.

4.1. Emulsion-Defined Droplets

The first experiment with single enzyme molecules was performed in 1961 by Rotman.[7] A solution of the enzyme β-galactosidase with the fluorogenic substrate 6-hydroxyfluoran-β-D-galactopyranoside was sprayed into silicone oil. The diameter of the resulting water-in-oil droplets was broadly distributed between 0.1 and 40 μm, but only those droplets with a diameter of 14–15 μm (1400 fL) were selected. The number of enzyme molecules in the droplets was calculated using the Poisson distribution. The reaction rates in these emulsion droplets were determined by comparing the accumulated fluorescent product 6-hydroxyfluoran to equally

sized droplets containing standard concentrations of 6-hydroxyfluoran. This study showed that heat inactivation yielded a mixture of active and inactive enzyme molecules rather than partially inactivating all enzyme molecules, a result that was essentially hidden in previous bulk experiments. At the time these experiments were conducted, the sensitivity of the methods limited the temporal resolution such that it was possible to measure the accumulated product only after 15 h.

Owing to the availability of modern CCD cameras, the substrate turnover of single chymotrypsin molecules confined in water-in-oil droplets could be measured in parallel with a time resolution of 8 min.[79] A maximum of one enzyme molecule per droplet was calculated for a droplet 1 μm in diameter. As the droplet sizes were again broadly distributed, larger droplets were discarded by the software. Smaller droplets were included in the calculation as they were less likely to contain more than one enzyme molecule. Chymotrypsin turns over the fluorogenic substrate $(sucAAPF)_2$-rhodamine 110 to fluorescent rhodamine 110. A limitation of this substrate, however, is its complicated reaction kinetics because each substrate molecule contains two cleavage sites for chymotrypsin. The formation of rhodamine 110 in water-in-oil droplets was not constant over time and showed variations among different chymotrypsin molecules.

4.2. Lipid Vesicles

Biotinylated lipid vesicles 100 nm in diameter (0.5 aL) with a narrow size distribution were tethered to the surface of a biotinylated lipid bilayer on glass through an avidin linkage to perform single-molecule experiments with Texas Red labeled adenylate kinase or tetramethylrhodamine-labeled bovine serum albumin (BSA).[80] The number of protein molecules in a vesicle was determined by observing sudden photobleaching steps in the fluorescence time traces. Only those vesicles that exhibited photobleaching as a single event contained a single protein molecule and were selected for single-molecule experiments. Polarization spectroscopy revealed that protein molecules inside the lipid vesicles and proteins in solution have similar motional freedom. This vesicle encapsulation technique was used to measure the conformational fluctuations of single adenylate kinase molecules in real time by using fluorescence resonance energy transfer (FRET) between two labels located in the core domain of the protein.[81] Folding and unfolding transitions were visible as correlated steps in donor and acceptor fluorescence intensity. This single-molecule experiment revealed that the size of these steps and the time scale of the transitions were broadly distributed.

Changing the solution inside surface-tethered lipid vesicles 200 nm in diameter was facilitated by membrane perforation with the bacterial toxin α-hemolysin or by incubating the vesicles near the melting temperature (T_m) to induce defects in the lipid packing.[82] This technique was used to investigate RecA protein of *E. coli* which stabilizes single-stranded DNA (ssDNA). Both ends of a ssDNA molecule were labeled with complementary FRET donor–acceptor dyes. RecA monomers assemble around ssDNA to form a filament, which stretches the naturally coiled ssDNA and pushes the FRET dyes apart, resulting in lower FRET efficiency. The concentrations were chosen to obtain on average one ssDNA molecule and approximately seven RecA molecules per vesicle. Dissociation of RecA from ssDNA depends on ATP hydrolysis. ATP was exchangeable through the membrane pores, while ssDNA and RecA could not pass. In this way, repetitive binding and dissociation of the same RecA filament on ssDNA was observed.

Optically trapped lipid vesicles with diameters of 3.3 to 11 μm (20–700 fL) were used to enclose single alkaline phosphatase molecules.[83] To select only vesicles with a single enzyme molecule, alkaline phosphatase was labeled with a fluorescent dye such that the number of enclosed enzyme molecules could be counted in a lipid vesicle. The fluorogenic substrate fluorescein diphosphate was confined in another vesicle. The contents of the different vesicles were then mixed by electrofusion. The reaction product fluorescein was detected by fluorescence microscopy, and the enzymatic rates were standardized with fluorescein-loaded liposomes. Individual alkaline phosphatase molecules exhibited long-lived (1 h) and broadly distributed activities, which were attributed to distinct conformational states.

4.3. Virus Capsids

Another format of biomimetic containers used for single-enzyme-molecule studies is the virus capsid (Figure 8).[84] Many viruses are covered by an icosahedral protein capsid with diameters from 12 to 500 nm.[85] The capsid of the cowpea chlorotic mottle virus (CCMV) has an inner diameter of 18 nm and thus defines a container of 3 zL volume. The CCMV capsid proteins were used for self-assembly around single molecules of horseradish peroxidase (HRP). Enclosed HRP molecules oxidized the nonfluorescent substrate dihydrorhodamine to the fluorescent product rhodamine, which was detected by confocal fluorescence microscopy. A confined volume of 3 zL containing substrate at a concentration of 0.5 μM would result in only one substrate molecule in every

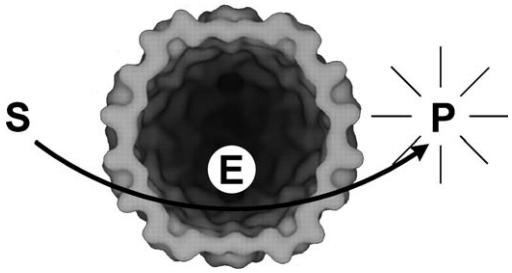

Figure 8. A single HRP molecule (E) enclosed in an icosahedral virus capsid. The substrate dihydrorhodamine (S) diffuses into the capsid where it is converted to the fluorescent product rhodamine (P). The fluorescent product accumulates before it finally diffuses out through capsid pores. Modified schematic representation reprinted with permission from Refs. [84] and [103].

thousand capsids. Thus, enzymatic reactions in confined zL volumes are not feasible. This limitation of confined zL containers was avoided by the size-selective permeability of the protein cage, which was used to keep the enzyme inside the capsid but allowed substrate and product to pass. Furthermore, the permeability of the capsid pores was pH dependent and could be used to control access of the substrate to the enzyme.

4.4. Capillary Electrophoresis

Capillary electrophoresis can be used for single-enzyme-molecule studies. In contrast to other fL container formats, a capillary confines a volume in only two directions but is open in the flow direction. Freely moving individual molecules of lactate dehydrogenase,[86] alkaline phosphatase,[87] or β-galactosidase[88] were electrophoretically separated along a capillary 10–20 μm in diameter that contained a fluorogenic substrate. The spacing of the individual enzyme molecules was adjusted such that the diffusion zones of the fluorescent product did not overlap. After a certain reaction time, the fluorescent product was electrophoretically moved to a fluorescence detector where the accumulated product of each individual enzyme molecule was measured quantitatively. Although the endpoint measurements cannot follow the kinetics of individual enzyme molecules, these experiments have another advantage. As the product and the enzyme molecules have different electrophoretic mobilities, they can be separated and the same enzyme can be used for a second incubation with fresh substrate or a different substrate. While each individual enzyme molecule had the same activity during repeated incubations, the activity among individual enzymes varied: in the case of lactate dehydrogenase the activity of different molecules varied by a factor of four. These differences were attributed to different long-lived conformational states of lactate dehydrogenase. β-Galactosidase from *E. coli* also showed a broad 20-fold activity distribution with the majority of molecules falling within a fourfold distribution. Crystallization of β-galactosidase for purification did not influence the wide activity distribution but reduced the average activity. The reaction rates of alkaline phosphatase, however, were heterogeneous only when the mammalian enzyme was used but homogeneous when the highly purified bacterial enzyme was used. These results were explained by posttranslational modifications, such as glycosylation, that are common for mammalian enzymes but do not occur in bacteria.

4.5. Lithographically Generated Arrays

Homogeneous arrays of fL and sub-fL containers can be fabricated directly on surfaces by lithographic techniques.[89] Electron beam lithography was used to fabricate arrays of holes 50 nm in diameter in a 100 nm metal film deposited on a glass coverslip.[90] The diameter of the holes was smaller than the wavelength of light such that light could not propagate into these "zero-mode waveguides", and fluorophores were excited only in the evanescent field at the glass–metal interface. DNA polymerase molecules were immobilized in the zero-mode waveguides with a maximum of one molecule per waveguide, and the enzymatic synthesis of double-stranded DNA was initiated by adding various fluorescent nucleotide triphosphates. The fluorescently labeled nucleotide analogues were detected upon sequential binding to the polymerase. Each time a fluorescent nucleotide was incorporated into a DNA strand, a burst of fluorescence was detected for a short time until the fluorescent dye photobleached or diffused away from the detection region. The evanescent field at the glass–metal interface effectively resulted in a zL observation volume such that the fluorescence background was greatly reduced. Thus, relatively high micromolar concentrations of the fluorescent nucleotides could be used, which is necessary for most polymerases to work efficiently. The holes in the metal film remained open to the substrate bulk solution, such that substrate depletion was avoided in such a small sub-fL reaction volume. This technique has been commercialized by Pacific Biosciences Inc. (Menlo Park, USA) for real-time DNA sequencing.[91]

Arrays of fL wells were microfabricated by photolithography into the surface of fused silica.[92] The semispherical wells 8 μm in diameter and 4 μm deep had a volume of 135 fL. The containers were filled by ultrasonication with vacuum degassing and sealed with a coverslip. Single molecules of lactate dehydrogenase (LDH-1) enclosed in the containers catalyzed the redox reaction of NAD^+ and lactate to give fluorescent NADH and pyruvate. This enzymatic reaction was compared to the reaction of a metal ion redox catalyst. Single Os^{VIII} ions catalyzed the redox reaction of Ce^{IV} and As^{III} to give fluorescent Ce^{III} and As^{V}. Both reactions were monitored by wide-field fluorescence microscopy. The activities of individual lactate dehydrogenase molecules differed by a factor of three while for individual metal ions, the observed activities were more similar. The broader activity distribution of the enzyme molecules was attributed to different conformations, which is not relevant for individual metal ions.

4.6. Optical-Fiber Bundles

In our laboratory, we enclosed individual *E. coli* β-galactosidase molecules in a homogenous array of 46 fL containers etched onto the surface of optical-fiber bundles.[93] β-Galactosidase converted the substrate resorufin-β-D-galactopyranoside in a single hydrolysis step to highly fluorescent resorufin (Figure 9). Resorufin was both excited and detected through the fiber bundle using wide-field fluorescence microscopy. Accurate kinetic rates were determined for hundreds of individual enzyme molecules. The fL containers enabled the small number of resorufin product molecules to build up to a detectable concentration while holding a sufficient number of resorufin-β-D-galactopyranoside molecules to avoid substrate depletion. Furthermore, photobleaching of the resorufin product was corrected by calculating the bleaching rate as measured with a resorufin standard solution. Observing a large population of individual β-galactosidase

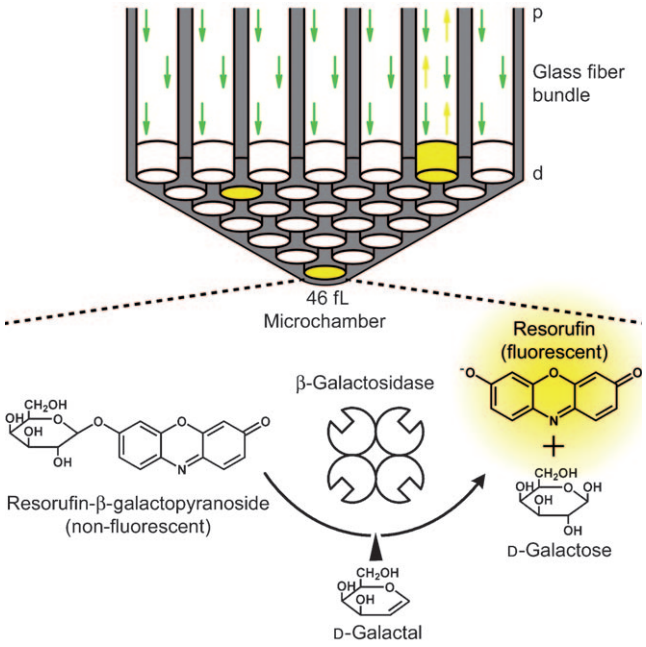

Figure 9. Single-enzyme-molecule experiment in an optical-fiber bundle array of 50000 fibers. Containers with a volume of 46 fL are etched homogenously into the distal end (d) of each fiber (fiber core: white, cladding: gray). The containers are sealed by a silicone gasket (not shown), and the reaction progress is monitored through the proximal side (p) of the fiber bundle by fluorescence microscopy. Individual enzyme molecules convert the nonfluorescent substrate resorufin-β-D-galactopyranoside to fluorescent resorufin (yellow containers). This process is inhibited when an inhibitor is bound to the enzyme. Schematic representation reprinted with permission from Ref. [96].

molecules in the optical-fiber array revealed distinct and long-lived substrate turnover rates that were broadly distributed.[94] This static heterogeneity was attributed to different conformational states of β-galactosidase. These results confirmed and went beyond previous single-molecule studies with β-galactosidase[88,92] because the activity distributions were analyzed at different substrate concentrations. As the normalized velocity distribution was found to be independent of the substrate concentration, we concluded that variability in the catalytic step k_{cat} is the source of the broad activity distribution.

While the substrate turnover rates of β-galactosidase were similar in the fL containers and in bulk solution, horseradish peroxidase (HRP) exhibited a 10 times lower rate of product formation at the single-molecule level than in bulk solution.[95] This reduced product formation rate in the fL containers can be explained by the particular redox reaction mechanism of HRP, which first oxidizes the fluorogenic substrate Amplex Red to nonfluorescent radical intermediates in a one-electron transfer step. Subsequently, two radical intermediates form the fluorescent product resorufin in an enzyme-independent dismutation reaction. If HRP is confined in a fL container, the rate of the dismutation reaction decreases and less product is formed.

β-Galactosidase was used to investigate for the first time competitive enzyme inhibition at the single-molecule level (Figure 9).[96] When the slow-binding inhibitor D-galactal was added to the enzyme/substrate solution in the fL containers on the optical-fiber bundle, binding and unbinding of D-galactal could be observed, leading to inhibited and active states of β-galactosidase, respectively. In a pre-steady-state experiment, β-galactosidase was first incubated with a concentration of D-galactal that was much higher than the inhibition constant K_i, then highly diluted, and enclosed in the fL array. A time-delayed onset of substrate turnover in the fL containers exhibited stochastic inhibitor release events. Although β-galactosidase is a tetramer with four subunits, upon activation, individual β-galactosidase molecules directly switched from zero to maximum activity. This observation can be explained by cooperative unbinding of D-galactal from the four subunits. Under steady-state conditions, when the enzyme was incubated with D-galactal at a concentration equal to K_i, monitoring the substrate turnover changes over long time periods revealed repeated inhibitor binding and unbinding events. The substrate turnover of an individual enzyme molecule changed after inhibitor release, indicating that D-galactal binding or unbinding is accompanied by conformational changes of the enzyme's catalytic sites. The rate constants derived from stochastic inhibitor binding and unbinding events were consistent with bulk reaction kinetics.

Single β-galactosidase molecules were also used as reporters for various single analyte molecules bound to the surface of the fL containers. The method involved amplifying a single-analyte-molecule binding event using an enzyme label. The principle was demonstrated with a biotin-derivatized container surface which efficiently captured single molecules of streptavidin-labeled β-galactosidase.[97] The enzyme was detected by sealing the fL containers and observing the accumulation of fluorescent resorufin. This technique is being developed by Quanterix Inc. (Cambridge, USA) for diagnostic applications. Proteins from human serum are captured on the container surface and labeled with β-galactosidase. The resulting high sensitivity is important because the concentration of many proteins is below the detection limit of current assays. Alternatively, single-stranded DNA molecules can be attached to the container surface of an optical-fiber bundle.[98] Upon hybridization with a biotinylated complementary DNA strand followed by binding of streptavidin-labeled β-galactosidase, single molecules of DNA were detectable at fM detection limits.

4.7. PDMS Devices

Identical PDMS sheets with arrays of 30 fL containers were molded iteratively with a silicon master stamp patterned by photolithography.[99] An enzyme–substrate solution was sandwiched between the PDMS mold and a glass plate. Gas bubbles and excess solution were evacuated from the fL containers by mechanical pressure, and adhesion of PDMS to the glass was sufficient to seal the containers. With this approach, single β-galactosidase molecules were investigated by observing the hydrolysis of the fluorescein-di-β-D-galactopyranoside substrate to the fluorescent product fluorescein using wide-field fluorescence microscopy. As a 1:1 ratio

between enzyme molecules and fL containers was used, some of the containers held more than a single β-galactosidase molecule. The distribution of enzyme activities in the fL containers was attributed to the different number of enzyme molecules occupying each container. This approach, however, obscured the wide activity differences of individual β-galactosidase molecules observed by other groups.[88,92,94] A fL array in PDMS was later combined with a microfluidic device to mix reactants in approximately 100 ms before they were enclosed in the fL containers with a glass coverslip.[100] The activity of single β-galactosidase molecules was observed using the substrate resorufin-β-D-galactopyranoside, which is hydrolyzed to highly fluorescent resorufin. The short dead times enabled the observation of single enzyme molecule reactions at early stages as well as at steady state. Another array with 4 fL containers in PDMS was recently used to investigate single α-chymotrypsin molecules with a quenched fluorophore–protein substrate.[101]

F_1-ATPase is a ubiquitous biological motor enzyme whose rotation is mechanochemically coupled to ATP hydrolysis or generation. A sophisticated combination of arrays with 6 fL containers in PDMS and F_1-ATP synthetase attached to a glass surface was used to investigate ATP hydrolysis and synthesis at the single-molecule level (Figure 10).[102] F_1-ATPase labeled with a magnetic bead was attached to the surface of a glass slide. Then, the glass was covered with the PDMS array such that only a single F_1-ATPase molecule was present in a given fL container. The magnetic bead on F_1-ATPase was rotated clockwise with magnetic tweezers to force ATP synthesis against a chemical potential in the fL containers. The containers were large enough to avoid physical interference with the rotating bead. When the magnetic field was turned off, the molecular motor rotated with the ATP gradient in an anticlockwise direction at a speed proportional to the amount of synthesized ATP. This single-molecule experiment confirmed that one revolution of the molecular motor involves three catalytic events with very high mechanochemical coupling.

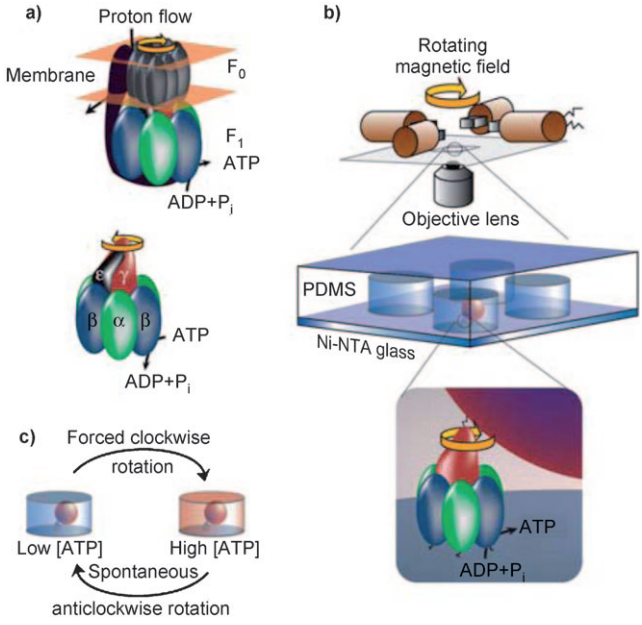

Figure 10. Single-molecule experiment with F_1-ATP synthase enclosed in a fL container. a) In the membrane-embedded F_0F_1-ATP synthase, the proton-driven F_0 rotates F_1 in a clockwise direction for ATP synthesis. b) A magnetic bead is connected to the surface-bound F_1-ATPase. Magnetic tweezers rotate the bead clockwise to drive ATP synthesis against a chemical potential. The PDMS array covers the glass such that only a single F_1-ATPase is present in a fL container. c) When the magnetic field is released, the molecular motor rotates with the ATP gradient in an anticlockwise direction at a speed proportional to the amount of synthesized ATP in the container. Schematic representation reprinted with permission from Ref. [102].

5. Summary and Outlook

In this review, we have discussed analytical applications of various fL and sub-fL container formats. Such containers are prepared either by self-assembly (bottom-up approach) or by surface patterning such as etching (top-down approach). This distinction, however, is not comprehensive, as, for example, nanofiber junctions do not fall into either category. Containers that form by self-assembly are emulsion droplets, lipid vesicles, or virus particles. Etching techniques can be used to generate open fL containers (or wells) on optical-fiber bundles, where the pattern of the fL wells is defined by the material, or by lithography, where the pattern is provided by a photolithographic mask. Alternatively, the etched surface can be used as a template for molding fL wells in PDMS. Surface-etched or molded wells can be filled repetitively with analytes, sensing elements, or cells. Because of the small feature size of fL containers, they can form very high density arrays. For example, arrays on optical-fiber bundles have a density of $\approx 25\,000\ mm^{-2}$. When these fL arrays are filled, thousands of analytical measurements can be made simultaneously on an area smaller than a pinhead.

Single-molecule studies on enzymes and other biomolecules are an emerging application of fL containers. Single-molecule experiments provide new perspectives on enzyme kinetics and mechanisms that are hidden in bulk experiments. Enclosing single enzyme molecules in fL containers requires no surface immobilization of the enzyme. Thus, the potential steric hindrance, partial inactivation, and perturbation of the enzyme structure associated with surface immobilization are avoided. Femtoliter containers have an ideal size for single-enzyme-molecule studies as they are small enough to isolate single enzyme molecules and can quickly accumulate a high product concentration. At the same time they are also large enough to hold a sufficient number of substrate molecules to prevent substrate depletion. Single-molecule experiments in fL containers rely on the availability of high-density arrays, as only a fraction of the containers can be used to preclude more than a single molecule from occupying a given container. Despite the need for a sparse occupation of the containers by single molecules, in large arrays hundreds to thousands of individual enzyme molecules can be monitored simultaneously.

Femtoliter arrays have been employed for making analytical measurements and for fundamental research on single-molecule kinetics. These two fields come together in single-

molecule sensing applications that enable a digital concentration readout of an analyte. These techniques include DNA sequencing with single DNA polymerase molecules in zero-mode waveguides[91] and amplifying a single-molecule binding event with an enzyme label in optical-fiber bundles.[97] While standard measurements indicate the concentration of an analyte by an analog response, single-molecule measurements exhibit a digital response to an analyte. This digital signal output has the potential to increase sensitivity since digital signals are noise-resistant owing to their binary nature.

Femtoliter arrays provide the opportunity to move the field of analytical chemistry into the ultimate realm of sensitivity—single-molecule detection. New engineering techniques for preparing large arrays of homogeneous ultrasmall containers promise rapid advances for fL analytical chemistry. We predict that fL analytical chemistry will displace some standard analytical methods in research laboratory settings as well as in a variety of commercial applications.

Received: November 13, 2009
Published online: April 23, 2010

[1] D. S. Goodsell, *Trends Biochem. Sci.* **1991**, *16*, 203 – 206.
[2] X. S. Xie, J. Yu, W. Y. Yang, *Science* **2006**, *312*, 228 – 230.
[3] D. T. Chiu, R. M. Lorenz, G. D. Jeffries, *Anal. Chem.* **2009**, *81*, 5111 – 5118.
[4] C. N. LaFratta, D. R. Walt, *Chem. Rev.* **2008**, *108*, 614 – 637.
[5] K. D. Bake, D. R. Walt, *Annu. Rev. Anal. Chem.* **2008**, *1*, 515 – 547.
[6] C. Auffray, Z. Chen, L. Hood, *Genome Med.* **2009**, *1*, 2.
[7] B. Rotman, *Proc. Natl. Acad. Sci. USA* **1961**, *47*, 1981 – 1991.
[8] D. M. Vriezema, M. C. Aragones, J. A. A. W. Elemans, J. J. L. M. Cornelissen, A. E. Rowan, R. J. M. Nolte, *Chem. Rev.* **2005**, *105*, 1445 – 1489.
[9] J. Bibette, F. L. Calderon, P. Poulin, *Rep. Prog. Phys.* **1999**, *62*, 969 – 1033.
[10] P. Becher, *Emulsions: Theory and Practice*, Oxford University Press, Oxford, UK, **2001**.
[11] M. Nakano, J. Komatsu, S. Matsuura, K. Takashima, S. Katsura, A. Mizuno, *J. Biotechnol.* **2003**, *102*, 117 – 124.
[12] R. Williams, S. G. Peisajovich, O. J. Miller, S. Magdassi, D. S. Tawfik, A. D. Griffiths, *Nat. Methods* **2006**, *3*, 545 – 550.
[13] a) M. Margulies, M. Egholm, W. E. Altman, S. Attiya, J. S. Bader, L. A. Bemben, J. Berka, M. S. Braverman, Y. J. Chen, Z. T. Chen, S. B. Dewell, L. Du, J. M. Fierro, X. V. Gomes, B. C. Godwin, W. He, S. Helgesen, C. H. Ho, G. P. Irzyk, S. C. Jando, M. L. I. Alenquer, T. P. Jarvie, K. B. Jirage, J. B. Kim, J. R. Knight, J. R. Lanza, J. H. Leamon, S. M. Lefkowitz, M. Lei, J. Li, K. L. Lohman, H. Lu, V. B. Makhijani, K. E. McDade, M. P. McKenna, E. W. Myers, E. Nickerson, J. R. Nobile, R. Plant, B. P. Puc, M. T. Ronan, G. T. Roth, G. J. Sarkis, J. F. Simons, J. W. Simpson, M. Srinivasan, K. R. Tartaro, A. Tomasz, K. A. Vogt, G. A. Volkmer, S. H. Wang, Y. Wang, M. P. Weiner, P. G. Yu, R. F. Begley, J. M. Rothberg, *Nature* **2005**, *437*, 376 – 380; b) J. Shendure, G. J. Porreca, N. B. Reppas, X. X. Lin, J. P. McCutcheon, A. M. Rosenbaum, M. D. Wang, K. Zhang, R. D. Mitra, G. M. Church, *Science* **2005**, *309*, 1728 – 1732.
[14] D. S. Tawfik, A. D. Griffiths, *Nat. Biotechnol.* **1998**, *16*, 652 – 656.
[15] A. V. Pietrini, P. L. Luisi, *ChemBioChem* **2004**, *5*, 1055 – 1062.
[16] M. Hashimoto, S. S. Shevkoplyas, B. Zasonska, T. Szymborski, P. Garstecki, G. M. Whitesides, *Small* **2008**, *4*, 1795 – 1805.
[17] S. L. Anna, N. Bontoux, H. A. Stone, *Appl. Phys. Lett.* **2003**, *82*, 364 – 366.
[18] C. Holtze, A. C. Rowat, J. J. Agresti, J. B. Hutchison, F. E. Angile, C. H. J. Schmitz, S. Koster, H. Duan, K. J. Humphry, R. A. Scanga, J. S. Johnson, D. Pisignano, D. A. Weitz, *Lab Chip* **2008**, *8*, 1632 – 1639.
[19] M. M. Kiss, L. Ortoleva-Donnelly, N. R. Beer, J. Warner, C. G. Bailey, B. W. Colston, J. M. Rothberg, D. R. Link, J. H. Leamon, *Anal. Chem.* **2008**, *80*, 8975 – 8981.
[20] L. Mazutis, A. F. Araghi, O. J. Miller, J. C. Baret, L. Frenz, A. Janoshazi, V. Taly, B. J. Miller, J. B. Hutchison, D. Link, A. D. Griffiths, M. Ryckelynck, *Anal. Chem.* **2009**, *81*, 4813 – 4821.
[21] P. Garstecki, M. J. Fuerstman, H. A. Stone, G. M. Whitesides, *Lab Chip* **2006**, *6*, 437 – 446.
[22] M. Y. He, J. S. Edgar, G. D. M. Jeffries, R. M. Lorenz, J. P. Shelby, D. T. Chiu, *Anal. Chem.* **2005**, *77*, 1539 – 1544.
[23] R. M. Lorenz, J. S. Edgar, G. D. M. Jeffries, D. T. Chiu, *Anal. Chem.* **2006**, *78*, 6433 – 6439.
[24] G. D. M. Jeffries, J. S. Kuo, D. T. Chiu, *Angew. Chem.* **2007**, *119*, 1348 – 1350; *Angew. Chem. Int. Ed.* **2007**, *46*, 1326 – 1328.
[25] J. Tang, A. M. Jofre, G. M. Lowman, R. B. Kishore, J. E. Reiner, K. Helmerson, L. S. Goldner, M. E. Greene, *Langmuir* **2008**, *24*, 4975 – 4978.
[26] M. Y. He, J. S. Kuo, D. T. Chiu, *Appl. Phys. Lett.* **2005**, *87*, 031916.
[27] a) S. Y. Teh, R. Lin, L. H. Hung, A. P. Lee, *Lab Chip* **2008**, *8*, 198 – 220; b) H. Song, D. L. Chen, R. F. Ismagilov, *Angew. Chem.* **2006**, *118*, 7494 – 7516; *Angew. Chem. Int. Ed.* **2006**, *45*, 7336 – 7356; c) A. Huebner, S. Sharma, M. Srisa-Art, F. Hollfelder, J. B. Edel, A. J. Demello, *Lab Chip* **2008**, *8*, 1244 – 1254.
[28] S. Prakash, A. Piruska, E. N. Gatimu, P. W. Bohn, J. V. Sweedler, M. A. Shannon, *IEEE Sens. J.* **2008**, *8*, 441 – 450.
[29] G. M. Whitesides, *Nat. Biotechnol.* **2003**, *21*, 1161 – 1165.
[30] Y. H. Zhang, P. Ozdemir, *Anal. Chim. Acta* **2009**, *638*, 115 – 125.
[31] F. Courtois, L. F. Olguin, G. Whyte, D. Bratton, W. T. S. Huck, C. Abell, F. Hollfelder, *ChemBioChem* **2008**, *9*, 439 – 446.
[32] P. S. Dittrich, M. Jahnz, P. Schwille, *ChemBioChem* **2005**, *6*, 811 – 814.
[33] I. G. Loscertales, A. Barrero, I. Guerrero, R. Cortijo, M. Marquez, A. M. Ganan-Calvo, *Science* **2002**, *295*, 1695 – 1698.
[34] J. B. Fenn, M. Mann, C. K. Meng, S. F. Wong, C. M. Whitehouse, *Science* **1989**, *246*, 64 – 71.
[35] A. Jesorka, O. Orwar, *Annu. Rev. Anal. Chem.* **2008**, *1*, 801 – 832.
[36] D. T. Chiu, C. F. Wilson, F. Ryttsen, A. Stromberg, C. Farre, A. Karlsson, S. Nordholm, A. Gaggar, B. P. Modi, A. Moscho, R. A. Garza-Lopez, O. Orwar, R. N. Zare, *Science* **1999**, *283*, 1892 – 1895.
[37] P. Y. Bolinger, D. Stamou, H. Vogel, *Angew. Chem.* **2008**, *120*, 5626 – 5631; *Angew. Chem. Int. Ed.* **2008**, *47*, 5544 – 5549.
[38] D. Stamou, C. Duschl, E. Delamarche, H. Vogel, *Angew. Chem.* **2003**, *115*, 5738 – 5741; *Angew. Chem. Int. Ed.* **2003**, *42*, 5580 – 5583.
[39] R. Karlsson, A. Karlsson, O. Orwar, *J. Am. Chem. Soc.* **2003**, *125*, 8442 – 8443.
[40] R. Karlsson, A. Karlsson, A. Ewing, P. Dommersnes, J. F. Joanny, A. Jesorka, O. Orwar, *Anal. Chem.* **2006**, *78*, 5960 – 5968.
[41] P. Anzenbacher, M. A. Palacios, *Nat. Chem.* **2009**, *1*, 80 – 86.
[42] a) P. Pantano, D. R. Walt, *Chem. Mater.* **1996**, *8*, 2832 – 2835; b) H. H. Gorris, T. M. Blicharz, D. R. Walt, *FEBS J.* **2007**, *274*, 5462 – 5470; c) D. R. Walt, *Chem. Soc. Rev.* **2010**, *39*, 38 – 50.
[43] a) S. Brenner, M. Johnson, J. Bridgham, G. Golda, D. H. Lloyd, D. Johnson, S. Luo, S. McCurdy, M. Foy, M. Ewan, R. Roth, D. George, S. Eletr, G. Albrecht, E. Vermaas, S. R. Williams, K. Moon, T. Burcham, M. Pallas, R. B. DuBridge, J. Kirchner, K.

Fearon, J. Mao, K. Corcoran, *Nat. Biotechnol.* **2000**, *18*, 630 – 634; b) J. M. Yeakley, J. B. Fan, D. Doucet, L. Luo, E. Wickham, Z. Ye, M. S. Chee, X. D. Fu, *Nat. Biotechnol.* **2002**, *20*, 353 – 358; c) D. R. Walt, *Science* **2000**, *287*, 451 – 452.
[44] R. Wilson, A. R. Cossins, D. G. Spiller, *Angew. Chem.* **2006**, *118*, 6250 – 6263; *Angew. Chem. Int. Ed.* **2006**, *45*, 6104 – 6117.
[45] J. A. Ferguson, F. J. Steemers, D. R. Walt, *Anal. Chem.* **2000**, *72*, 5618 – 5624.
[46] K. L. Gunderson, S. Kruglyak, M. S. Graige, F. Garcia, B. G. Kermani, C. Zhao, D. Che, T. Dickinson, E. Wickham, J. Bierle, D. Doucet, M. Milewski, R. Yang, C. Siegmund, J. Haas, L. Zhou, A. Oliphant, J. B. Fan, S. Barnard, M. S. Chee, *Genome Res.* **2004**, *14*, 870 – 877.
[47] L. N. Song, S. Ahn, D. R. Walt, *Anal. Chem.* **2006**, *78*, 1023 – 1033.
[48] S. Ahn, D. R. Walt, *Anal. Chem.* **2005**, *77*, 5041 – 5047.
[49] S. Ahn, D. M. Kulis, D. L. Erdner, D. M. Anderson, D. R. Walt, *Appl. Environ. Microbiol.* **2006**, *72*, 5742 – 5749.
[50] D. M. Rissin, D. R. Walt, *Anal. Chim. Acta* **2006**, *564*, 34 – 39.
[51] T. Konry, R. B. Hayman, D. R. Walt, *Anal. Chem.* **2009**, *81*, 5777 – 5782.
[52] a) V. M. Mirsky, T. Hirsch, S. A. Piletsky, O. S. Wolfbeis, *Angew. Chem.* **1999**, *111*, 1179 – 1181; *Angew. Chem. Int. Ed.* **1999**, *38*, 1108 – 1110; b) T. Hirsch, H. Kettenberger, O. S. Wolfbeis, V. M. Mirsky, *Chem. Commun.* **2003**, 432 – 433.
[53] T. A. Dickinson, K. L. Michael, J. S. Kauer, D. R. Walt, *Anal. Chem.* **1999**, *71*, 2192 – 2198.
[54] S. E. Stitzel, L. J. Cowen, K. J. Albert, D. R. Walt, *Anal. Chem.* **2001**, *73*, 5266 – 5271.
[55] a) K. J. Albert, D. R. Walt, D. S. Gill, T. C. Pearce, *Anal. Chem.* **2001**, *73*, 2501 – 2508; b) K. J. Albert, D. R. Walt, *Anal. Chem.* **2000**, *72*, 1947 – 1955.
[56] M. J. Aernecke, J. Guo, S. Sonkusale, D. R. Walt, *Anal. Chem.* **2009**, *81*, 5281 – 5290.
[57] S. Köster, F. E. Angile, H. Duan, J. J. Agresti, A. Wintner, C. Schmitz, A. C. Rowat, C. A. Merten, D. Pisignano, A. D. Griffiths, D. A. Weitz, *Lab Chip* **2008**, *8*, 1110 – 1115.
[58] J. C. Baret, O. J. Miller, V. Taly, M. Ryckelynck, A. El-Harrak, L. Frenz, C. Rick, M. L. Samuels, J. B. Hutchison, J. J. Agresti, D. R. Link, D. A. Weitz, A. D. Griffiths, *Lab Chip* **2009**, *9*, 1850 – 1858.
[59] H. N. Joensson, M. L. Samuels, E. R. Brouzes, M. Medkova, M. Uhlen, D. R. Link, H. Andersson-Svahn, *Angew. Chem.* **2009**, *121*, 2556 – 2559; *Angew. Chem. Int. Ed.* **2009**, *48*, 2518 – 2521.
[60] J. Q. Boedicker, L. Li, T. R. Kline, R. F. Ismagilov, *Lab Chip* **2008**, *8*, 1265 – 1272.
[61] a) Y. Kuang, I. Biran, D. R. Walt, *Anal. Chem.* **2004**, *76*, 2902 – 2909; b) Y. Kuang, I. Biran, D. R. Walt, *Anal. Chem.* **2004**, *76*, 6282 – 6286.
[62] R. D. Whitaker, D. R. Walt, *Anal. Biochem.* **2007**, *360*, 63 – 74.
[63] L. C. Taylor, D. R. Walt, *Anal. Biochem.* **2000**, *278*, 132 – 142.
[64] R. D. Whitaker, D. R. Walt, *Anal. Chem.* **2007**, *79*, 9045 – 9053.
[65] I. Biran, D. R. Walt, *Anal. Chem.* **2002**, *74*, 3046 – 3054.
[66] Y. Kuang, I. Biran, D. R. Walt, *Anal. Chem.* **2004**, *76*, 6282 – 6286.
[67] S. Yamamura, H. Kishi, Y. Tokimitsu, S. Kondo, R. Honda, S. R. Rao, M. Omori, E. Tamiya, A. Muraguchi, *Anal. Chem.* **2005**, *77*, 8050 – 8056.
[68] a) Y. N. Xia, G. M. Whitesides, *Annu. Rev. Mater. Sci.* **1998**, *28*, 153 – 184; b) Y. N. Xia, G. M. Whitesides, *Angew. Chem.* **1998**, *110*, 568 – 594; *Angew. Chem. Int. Ed.* **1998**, *37*, 550 – 575.
[69] J. R. Rettig, A. Folch, *Anal. Chem.* **2005**, *77*, 5628 – 5634.
[70] Y. Sasuga, T. Iwasawa, K. Terada, Y. Oe, H. Sorimachi, O. Ohara, Y. Harada, *Anal. Chem.* **2008**, *80*, 9141 – 9149.
[71] J. Q. Boedicker, M. E. Vincent, R. F. Ismagilov, *Angew. Chem.* **2009**, *121*, 6022 – 6025; *Angew. Chem. Int. Ed.* **2009**, *48*, 5908 – 5911.
[72] a) X. S. Xie, P. J. Choi, G. W. Li, N. K. Lee, G. Lia, *Annu. Rev. Biophys.* **2008**, *37*, 417 – 444; b) J. Elf, G. W. Li, X. S. Xie, *Science* **2007**, *316*, 1191 – 1194; c) I. Golding, J. Paulsson, S. M. Zawilski, E. C. Cox, *Cell* **2005**, *123*, 1025 – 1036; d) J. Yu, J. Xiao, X. J. Ren, K. Q. Lao, X. S. Xie, *Science* **2006**, *311*, 1600 – 1603; e) K. P. Lemon, A. D. Grossman, *Science* **1998**, *282*, 1516 – 1519.
[73] M. Böhmer, J. Enderlein, *ChemPhysChem* **2003**, *4*, 792 – 808.
[74] a) L. Edman, Z. Földes-Papp, S. Wennmalm, R. Rigler, *Chem. Phys.* **1999**, *247*, 11 – 22; b) B. P. English, W. Min, A. M. van Oijen, K. T. Lee, G. Luo, H. Sun, B. J. Cherayil, S. C. Kou, X. S. Xie, *Nat. Chem. Biol.* **2006**, *2*, 87 – 94; c) A. M. van Oijen, P. C. Blainey, D. J. Crampton, C. C. Richardson, T. Ellenberger, X. S. Xie, *Science* **2003**, *301*, 1235 – 1238; d) K. Velonia, O. Flomenbom, D. Loos, S. Masuo, M. Cotlet, Y. Engelborghs, J. Hofkens, A. E. Rowan, J. Klafter, R. J. M. Nolte, F. C. de Schryver, *Angew. Chem.* **2005**, *117*, 566 – 570; *Angew. Chem. Int. Ed.* **2005**, *44*, 560 – 564.
[75] H. P. Lu, L. Xun, X. S. Xie, *Science* **1998**, *282*, 1877 – 1882.
[76] R. M. Dickson, A. B. Cubitt, R. Y. Tsien, W. E. Moerner, *Nature* **1997**, *388*, 355 – 358.
[77] W. L. Xu, J. S. Kong, P. Chen, *J. Phys. Chem. C* **2009**, *113*, 2393 – 2404.
[78] X. Michalet, S. Weiss, M. Jager, *Chem. Rev.* **2006**, *106*, 1785 – 1813.
[79] A. I. Lee, J. P. Brody, *Biophys. J.* **2005**, *88*, 4303 – 4311.
[80] E. Boukobza, A. Sonnenfeld, G. Haran, *J. Phys. Chem. B* **2001**, *105*, 12165 – 12170.
[81] E. Rhoades, E. Gussakovsky, G. Haran, *Proc. Natl. Acad. Sci. USA* **2003**, *100*, 3197 – 3202.
[82] I. Cisse, B. Okumus, C. Joo, T. J. Ha, *Proc. Natl. Acad. Sci. USA* **2007**, *104*, 12646 – 12650.
[83] T. M. Hsin, E. S. Yeung, *Angew. Chem.* **2007**, *119*, 8178 – 8181; *Angew. Chem. Int. Ed.* **2007**, *46*, 8032 – 8035.
[84] M. Comellas-Aragonès, H. Engelkamp, V. I. Claessen, N. A. J. M. Sommerdijk, A. E. Rowan, P. C. M. Christianen, J. C. Maan, B. J. M. Verduin, J. J. L. M. Cornelissen, R. J. M. Nolte, *Nat. Nanotechnol.* **2007**, *2*, 635 – 639.
[85] A. de La Escosura, R. J. M. Nolte, J. J. L. M. Cornelissen, *J. Mater. Chem.* **2009**, *19*, 2274 – 2278.
[86] a) Q. F. Xue, E. S. Yeung, *Anal. Chem.* **1994**, *66*, 1175 – 1178; b) Q. Xue, E. S. Yeung, *Nature* **1995**, *373*, 681 – 683.
[87] a) D. B. Craig, E. A. Arriaga, J. C. Y. Wong, H. Lu, N. J. Dovichi, *J. Am. Chem. Soc.* **1996**, *118*, 5245 – 5253; b) R. Polakowski, D. B. Craig, A. Skelley, N. J. Dovichi, *J. Am. Chem. Soc.* **2000**, *122*, 4853 – 4855.
[88] a) D. Craig, E. A. Arriaga, P. Banks, Y. Zhang, A. Renborg, M. M. Palcic, N. J. Dovichi, *Anal. Biochem.* **1995**, *226*, 147 – 153; b) D. B. Craig, N. J. Dovichi, *Can. J. Chem.* **1998**, *76*, 623 – 626; c) D. B. Craig, J. T. Nachtigall, H. L. Ash, G. K. Shoemaker, A. C. Dyck, T. M. Wawrykow, H. L. Gudbjartson, *J. Protein Chem.* **2003**, *22*, 555 – 561; d) G. K. Shoemaker, D. H. Juers, J. M. L. Coombs, B. W. Matthews, D. B. Craig, *Biochemistry* **2003**, *42*, 1707 – 1710.
[89] B. D. Gates, Q. Xu, M. Stewart, D. Ryan, C. G. Willson, G. M. Whitesides, *Chem. Rev.* **2005**, *105*, 1171 – 1196.
[90] M. J. Levene, J. Korlach, S. W. Turner, M. Foquet, H. G. Craighead, W. W. Webb, *Science* **2003**, *299*, 682 – 686.
[91] J. Eid, A. Fehr, J. Gray, K. Luong, J. Lyle, G. Otto, P. Peluso, D. Rank, P. Baybayan, B. Bettman, A. Bibillo, K. Bjornson, B. Chaudhuri, F. Christians, R. Cicero, S. Clark, R. Dalal, A. Dewinter, J. Dixon, M. Foquet, A. Gaertner, P. Hardenbol, C. Heiner, K. Hester, D. Holden, G. Kearns, X. Kong, R. Kuse, Y. Lacroix, S. Lin, P. Lundquist, C. Ma, P. Marks, M. Maxham, D. Murphy, I. Park, T. Pham, M. Phillips, J. Roy, R. Sebra, G. Shen, J. Sorenson, A. Tomaney, K. Travers, M. Trulson, J. Vieceli, J.

Wegener, D. Wu, A. Yang, D. Zaccarin, P. Zhao, F. Zhong, J. Korlach, S. Turner, *Science* **2009**, *323*, 133 – 138.
[92] W. H. Tan, E. S. Yeung, *Anal. Chem.* **1997**, *69*, 4242 – 4248.
[93] D. M. Rissin, D. R. Walt, *Nano Lett.* **2006**, *6*, 520 – 523.
[94] D. M. Rissin, H. H. Gorris, D. R. Walt, *J. Am. Chem. Soc.* **2008**, *130*, 5349 – 5353.
[95] H. H. Gorris, D. R. Walt, *J. Am. Chem. Soc.* **2009**, *131*, 6277 – 6282.
[96] H. H. Gorris, D. M. Rissin, D. R. Walt, *Proc. Natl. Acad. Sci. USA* **2007**, *104*, 17680 – 17685.
[97] D. M. Rissin, D. R. Walt, *J. Am. Chem. Soc.* **2006**, *128*, 6286 – 6287.
[98] Z. Li, R. B. Hayman, D. R. Walt, *J. Am. Chem. Soc.* **2008**, *130*, 12622 – 12623.
[99] Y. Rondelez, G. Tresset, K. V. Tabata, H. Arata, H. Fujita, S. Takeuchi, H. Noji, *Nat. Biotechnol.* **2005**, *23*, 361 – 365.
[100] S. Y. Jung, Y. Liu, C. P. Collier, *Langmuir* **2008**, *24*, 4439 – 4442.
[101] A. Y. Chen, A. S. Jani, L. Zheng, P. J. Burke, J. P. Brody, *Biotechnol. Prog.* **2009**, *25*, 929 – 937.
[102] Y. Rondelez, G. Tresset, T. Nakashima, Y. Kato-Yamada, H. Fujita, S. Takeuchi, H. Noji, *Nature* **2005**, *433*, 773 – 777.
[103] T. Douglas, M. Young, *Science* **2006**, *312*, 873 – 875.

